Temporal characteristics of global form perception in translational and circular Glass patterns

Temporal characteristics of global form perception in translational and circular Glass patterns

Rita Donato[1,2,3,†*], Andrea Pavan[4,†], Jorge Almeida[3,5], Massimo Nucci[1], and Gianluca Campana[1,2]

[1]University of Padova, Department of General Psychology, Via Venezia 8, 35131 Padova, Italy

[2]Human Inspired Technology Research Centre, University of Padova, Via Luzzati 4, 35121 Padova, Italy

[3]Proaction Laboratory, University of Coimbra, Faculty of Psychology and Educational Sciences, Colégio de Jesus, Rua Inácio Duarte 65, 3000-481 Coimbra, Portugal

[4]University of Bologna, Department of Psychology, Viale Berti Pichat, 5, 40127, Bologna, Italy

[5]CINEICC, University of Coimbra, Faculty of Psychology and Educational Sciences, Rua Colégio Novo, 3000-115 Coimbra, Portugal

***Corresponding Author**

Rita Donato

University of Padova

Department of General Psychology

Via Venezia 8, 35131 Padova, Italy

Tel: +39 (0)49 8276957

Email: rita.donato.phd@gmail.com

[†]The two authors contributed equally to the manuscript.

Abstract

The human visual system is continuously exposed to a natural environment with static and moving objects that the visual system needs to continuously integrate and process. Glass patterns (GPs) are a class of visual stimuli widely used to study how the human visual system processes and integrates form and motion signals. GPs are made of pairs of dots that elicit a strong percept of global form. A rapid succession of unique frames originates dynamic GPs. Previous psychophysical studies showed that dynamic translational GPs are easier to detect than the static version because of the spatial summation across the unique frames composing the pattern. However, it is not clear whether the same mechanism is involved in dynamic circular GPs. In the present study, we psychophysically investigated the role of the temporal and spatial summation in the perception of both translational and circular GPs. We manipulated the number of unique frames in dynamic GPs and the update rate of the frames presentation. The results suggest that spatial and temporal summation across unique frames takes place for both translational and circular GPs. Moreover, the number of unique frames and the pattern update rate equally influence the discrimination thresholds of translational and circular GPs. These results show that form and motion integration is likely to be processed similarly for translational and circular GPs.

Keywords: Translational Glass patterns, circular Glass patterns, dynamic Glass patterns, form-motion interaction, temporal summation, apparent motion

1. Introduction

Glass patterns (GPs) (Glass, 1969) are visual patterns widely used in psychophysical research to study how form and motion mechanisms interact in human and non-human primates' visual cortex (Kourtzi et al., 2005, 2008; Krekelberg et al., 2003, 2005; Lewis et al., 2002; Wilson et al., 2003, 2004; Wilson & Wilkinson, 1998). GPs are composed of dot pairs (dipoles) whose orientations align to create a global form; by applying different geometric transformations, it is possible to change the spatial relationship between dipole orientations to create visual textures that convey the perception of specific global forms such as radial, circular, or spiral patterns.

GPs can be static and dynamic. Static GPs are made of a single unique frame, whereas dynamic GPs are made of multiple independent frames, each containing a GP with randomly placed dipoles showed in rapid succession. Usually, for each new frame, a new spatial arrangement of the dipoles is created while the orientation remains constant. In dynamic GPs, the rapid succession of frames induces the perception of apparent motion along the pattern's orientation axis even though there is no dipole-to-dipole correspondence between successive frames. Therefore, no coherent motion is present in this class of stimuli (Nankoo et al., 2012; Pavan et al., 2017; Ross, Badcock & Hayes, 2000). In general, dynamic GPs are more easily detected and discriminated than static GPs (Burr & Ross, 2006; Nankoo et al., 2012, 2015; Or et al., 2007; Pavan et al., 2017, 2019). For static patterns, circular GPs exhibit lower detection or discrimination thresholds than translational GPs, a finding that has been attributed to the activity of concentrically tuned units in cortical area V4 (Wilson, Wilkinson, & Asaad, 1997; Wilson & Wilkinson, 1998). However, Dakin and Bex (2002) showed that the advantage of circular GPs over translational GPs may be due to the strong influence of the pattern edge (i.e., the aperture window) rather than the intrinsic statistical properties of the pattern. Dakin and Bex (2002) found that higher thresholds for translational GPs were correlated with the unmatched circular aperture of the patterns. On the other hand, Anderson and Swettenham (2006) using circular, radial, and translational (horizontal) GPs within a square aperture, found that both strabismic amblyopes and control participants showed a better detection performance for radial and circular GPs than translational GPs. Similarly, Kelly et al. (2001) measured the detection thresholds of circular, radial, and translational (vertical and horizontal) GPs, all presented in a square aperture. The authors found that participants better discriminated circular and radial GPs than translational GPs, despite the square aperture. Therefore, most of the studies report that the aperture window of GPs does not influence participants' detection thresholds.

Ostwald et al. (2008) using fMRI and different GP types presented in circular apertures, showed a continuum in the integration process from selectivity for local orientation signals in early visual areas, to selectivity for global form in higher occipitotemporal areas. Using multivoxel

pattern analysis (MVPA) the authors found that high-level occipitotemporal areas distinguish differences in global form, rather than low-level stimulus properties, with higher accuracy than early visual areas, consistent with the hypothesis of global pooling mechanisms of local orientation signals. Besides, classification accuracy in early visual areas (e.g., V1 and V2) was similar for all the GPs used (translational, radial, and concentric patterns), though the lateral occipital complex (LOC) exhibited higher classification accuracy for all the patterns.

Apparent motion evoked by dynamic GPs has been explored by various studies (Day & Palomares, 2014; Donato et al., 2020; Nankoo et al., 2012, 2015; Pavan et al., 2017; Ross, 2004). For example, Ross et al. (2000) found that the perception of apparent trajectory in dynamic GPs is particularly evident at high pattern update rates (i.e., when frames are presented in rapid succession). Moreover, the authors showed that the apparent motion in dynamic GPs is created by integrating form information in the dipoles among frames. Interestingly, there is neuroimaging evidence that shows that the human brain, in particular the human motion complex hMT+, responds similarly to apparent/non-directional motion generated by form cues and real/directional motion generated by motion cues, a feature called '*cue invariance*' (Krekelberg et al., 2005).

Furthermore, Day and Palomares (2014) investigated whether the change of the update rate in dynamic circular GPs affected global form perception. They used six different update rates (i.e., 1, 2, 4, 8, 18, and 36 Hz). Participants had to discriminate whether the coherent circular GP was presented in either the first or second temporal interval (two-interval forced-choice task; 2IFC task). The authors found that an increased update rate in dynamic GPs was correlated to improved participants' performance in GP detection. In conclusion, the temporal features of dynamic GPs are fundamental for the perception of apparent/non-directional motion. This finding supports the idea that temporal and form information (i.e., dipoles' orientation) in GPs is summed to increase the observer's sensitivity to the dynamic GPs.

Subsequently, Nankoo et al. (2012) assessed the detection thresholds of apparent and real motion generated by different types of GPs and random dot kinematograms (RDKs). The authors estimated and compared detection thresholds for radial, translational (horizontal and vertical), concentric and spiral patterns for static and dynamic GPs and RDKs. The results showed lower detection thresholds for dynamic GPs and RDKs than static GPs. However, detection thresholds of dynamic GPs had a similar trend to static GPs instead of RDKs. These results suggest that both types of GPs seem to be processed mainly by their form cues. This points to different neural mechanisms underlying GPs and RDKs. A possible reason why dynamic GPs have lower detection or discrimination thresholds than static GPs is that as soon as the update rate of dynamic GP increases, the number of frames also increases (Day & Palomares, 2014). This might induce a

temporal summation of local signals into a global percept that favors detection and discrimination processes. However, it remained unclear whether the enhanced sensitivity of dynamic GPs is to be attributed only to the temporal integration of local signals of the visual pattern (producing apparent and non-directional motion) or also to the summation of form signals occurring across multiple frames. This has been further investigated by Nankoo et al. (2015) in a psychophysical experiment where the authors used static and dynamic translational GPs. The rationale was that if the lower thresholds observed for dynamic GPs are due to the summation of multiple form signals, a linear decrease in threshold would be expected as the number of frames increases. Furthermore, given that each GP in the sequence producing dynamic GPs is presented for a short duration with respect to the single GP in the static pattern, the authors measured discrimination thresholds for GPs that contained blocks of unique frames. The authors used eight different types of dynamic translational GPs, where the combination between the number of unique frames (maximum 12 frames) and the update rate (maximum 60 Hz) was manipulated. Participants had to perform a 2IFC task in which they had to report whether the coherent translational GP was either in the first or second temporal interval. Their study aimed to test whether the lower discrimination thresholds for dynamic GPs were associated not only with high update rates, as found previously by Day and Palomares (2014), but also with a specific number of unique frames composing the GPs. The hypothesis was that if the perception of dynamic GPs is driven by form information summation, then it should be observed increased sensitivity of dynamic GPs as the number of unique frames increases. The authors showed that dynamic GPs with more unique frames are easier to discriminate because of the temporal summation of local signals. The authors chose to use translational GPs and no other spatial configurations because Nankoo et al. (2012) showed a more evident difference between discrimination thresholds for translational static and dynamic GPs than between other configurations such as spiral, radial, and circular. In other terms, using translational GPs, the divergence between GPs with a different number of unique frames and temporal frequencies should be more evident than other GPs configurations. These results confirmed that participants could better discriminate (i.e., lower coherence thresholds) dynamic translational GPs with twelve frames and an update rate of 60 Hz than with a lower number of frames, even if the resulting temporal frequency was the same. However, the authors concluded that motion mechanisms could also contribute to the better discrimination of dynamic translational GPs.

In this study, we examined whether global form signal in dynamic circular and translational GPs is integrated across frames and whether this facilitates participants' discrimination of dynamic GPs. Specifically, we aimed at investigating the mechanisms underlying the coding of both static and dynamic GPs for translational and circular configurations. This was tested by using the method

of Nankoo et al. (2015) with the same combination of unique frames and pattern update rates to assess whether there are overlapping mechanisms between the processing of simple (translational) and complex (circular) GP configurations. The present study aims to investigate whether participants' discrimination coherence thresholds for translational and circular GPs rely either on the number of unique frames that form dynamic GPs or on the pattern update rate independently from the number of unique frames. If the participants' sensitivity to GPs depends exclusively on the number of unique frames used, this could indicate summation of multiple form signals across frames (Nankoo et al., 2015). Therefore, as in Nankoo et al. (2015), we expect a linear decrease in discrimination thresholds as the number of unique frames increases. In the second case, if participants' sensitivity depends on the pattern update rate, this could indicate the temporal integration of local motion signals. We should expect a linear decrease of the discrimination threshold as the pattern update rate increases regardless of the number of unique frames involved. Moreover, we expect to observe lower discrimination thresholds for circular GPs than translational GPs throughout all the conditions, regardless of the number of unique frames and the pattern update rate. This expectation is based on previous studies (Lee & Lu, 2010, Nankoo et al., 2012; Rampone & Makin, 2020; Wilson & Wilkinson, 1998), which found that human observers are more sensitive to complex GPs (e.g., circular and radial patterns) than simple translational GPs.

2. Method

2.1. Participants

Twenty participants took part in the experiment. This sample size was established a priori using G*Power (Faul et al., 2007, 2009; Mayr et al., 2007) to achieve a power > 0.9 with an effect size of 0.25. All participants had normal or corrected to normal vision. In the experiment, viewing was binocular. All participants took part in two sessions on two different days (i.e., a session with translational GPs and another session with circular GPs). Participants were thirteen females and seven males with a mean age of 25 yrs. (SD: 7.33 yrs.). Two of the authors (RD and AP) performed the experiment; all the other participants were *naïve* to the study's purposes. Participants were informed about the research's general aim, and they signed a written informed consent prior the enrollment to the experiment. The experiment was run in agreement with the World Medical Association Declaration of Helsinki (2013). The study was approved by the Ethics Committee of the Faculty of Psychology and Educational Sciences of the University of Coimbra.

204 *2.2. Apparatus*

205 Visual stimuli were displayed on a 23.8-inch Hp Elite E240 monitor with a spatial resolution
206 of 1920 x 1080 pixel and a refresh rate of 60 Hz. Each pixel subtended ~1.65 arcmin. All
207 participants sat in a dimly light room at a viewing distance of 57 cm from the screen. Visual stimuli
208 were presented using Matlab Psychtoolbox-3 (http://psychtoolbox.org/) (Brainard, 1997; Kleiner et
209 al., 2007; Pelli, 1997).

210

211 *2.3. Stimuli*

212 The visual stimuli used in the experiment were translational and circular GPs (see Figure 1).
213 Both translational and circular GPs were characterized by 2146 white dipoles (density: 6%)
214 presented on a black background (Nankoo et al., 2015). The dot separation was 0.25 deg, and each
215 dot had a diameter of 0.04 deg. GPs were presented in a circular window within an annulus with a
216 maximum radius of 5.35 deg (diameter: 10.7 deg). Static GPs were composed of a single unique
217 frame, whereas dynamic GPs were made of multiple independent frames presented in rapid
218 succession (each frame had a duration of 0.0167-s). The duration of the stimulus was 0.2-s. The
219 sequence and number of unique frames (and relative pattern update rate) composing static and
220 dynamic GPs are reported in Table 1 (Nankoo et al., 2015). It should be noted that in condition 1
221 (i.e., the same 12 unique frames) the GPs, being presented for 0.2-s, have an update rate of 5 Hz and
222 are perceived as static patterns. At the center of the annulus, a white fixation point with a diameter
223 of 0.3 deg was always present.

224

Condition	Sequence of Unique Frames	Number of Unique Frames	Pattern Update Rate (Hz)
1	AAAAAAAAAAAA	1	5
2	ABCDEFGHIJKL	12	60
3	AAAAAABBBBBB	2	10
4	AAABBBAAABBB	2	20
5	ABABABABABAB	2	60
6	AAABBBCCCDDD	4	20
7	ABCDABCDABCD	4	60
8	AABBCCDDEEFF	6	30

Table 1. Summary of the conditions used in the experiment. Number of unique frames, frame sequences and pattern update rates used in the experiment are reported. The letters reported in the second column indicate the sequence of unique frames. Each participant performed all the nine conditions with the two types of GPs: circular and translational GPs. This scheme is the same as in Nankoo et al. (2015).

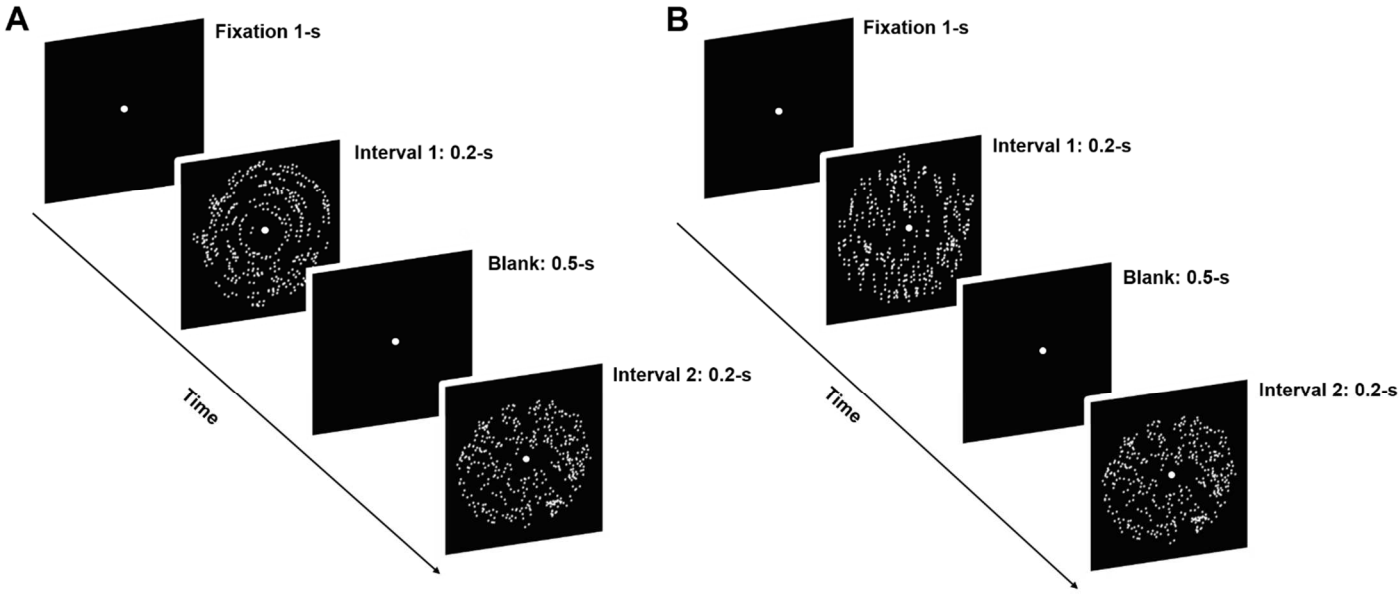

Figure 1. Representation of the visual stimuli and the procedure used in the experiment. Two temporal intervals of 0.2-s with a circular GP (A) or a translational GP (B) were presented after 1-s fixation. Panel A and B show respectively a circular and a translational GP with 100% coherence in the first temporal interval and a GP with 0% coherence (i.e., noise pattern) in the second temporal interval.

3. Procedure

Participants performed two sessions of two hours each and on two different days. The two sessions had the same procedure but differed for the type of visual stimulus used, i.e., either translational or circular GPs. The order of the two sessions was alternated amongst the participants. At the beginning of each session, each participant was instructed about the type of GP presented and they performed twenty trials to familiarize with the stimulus and task. During the training phase, one interval contained a GP with maximum coherence (100%) and the other interval a GP with randomly oriented dipoles (i.e., noise GP – 0% coherence). Each trial started with a fixation point of 1-s, followed by two 0.2-s temporal intervals separated by a blank interval of 0.5-s. One of

the two intervals always contained a coherent GP (either translational or circular, depending on the session) and the other interval a noise GP. The presentation order of the two intervals was randomized across trials. Observers performed a 2IFC task and had to report whether the first or second interval contained the coherent GP using the key "A" to indicate the first temporal interval and the key "L" to indicate the second temporal interval, on a standard Portuguese computer keyboard.

An Updated Maximum-Likelihood (UML) staircase procedure was used with a 1 up – 3 down rule to estimate participants' parameters of the psychometric function (Shen & Richards, 2012; Shen, Dai, & Richards, 2014). In this case, the threshold corresponds to a coherence level for which participants were at 79% correct performance.

The UML procedure allows efficient data collection to estimate the parameters of the psychometric function using an optimized strategy for stimulus sampling (Shen & Richards, 2012). In our implementation of the UML procedure, the Cumulative Gaussian was selected as psychometric function and had the following form:

$$p(correct) = \gamma + (1-\gamma-\lambda)\frac{1}{2}\left[1 + erf\left(\frac{x-\alpha}{\sqrt{2\beta^2}}\right)\right] \quad \text{Eq. 1}$$

where α is the center of the psychometric function, β is associated with the slope of the psychometric function, γ is the proportion correct for chance performance that in our case was fixed at 0.5, which set the lower bound of the psychometric function, and λ is the difference between the upper asymptote of the function and one, indicating the lapses rate.

The initial signal strength, i.e., number of coherently oriented dipoles, was set at 1800 dipoles, with limits in the interval [100 2000]. The range of the parameter α (i.e., coherence threshold) was in the interval [200 1900], with a prior uniform distribution. The range of the parameter β was in the interval [0.05 20] with a prior uniform distribution. The range of the parameter λ was in the interval [0 0.1], again with a prior uniform distribution. For each participant, the coherence threshold was calculated from the best parameters of the Cumulative Gaussian estimated with the UML procedure, finding the coherence corresponding to the 79% correct performance from the psychometric function. The slope of the Cumulative Gaussian function, calculated at the coherence threshold, can be derived as follows:

$$s = \frac{1-\gamma-\lambda}{\sqrt{2\pi\beta^2}} \quad \text{Eq. 2}$$

In both sessions, participants perform all the nine conditions (see Table 1), randomized among the participants and throughout the sessions. Each condition (and UML staircase) consisted of 150 trials.

4. Results

4.1. Discrimination thresholds

Discrimination thresholds for dynamic circular GPs (12 frames; 60 Hz) (mean: 18%, SD: 7.23%) were significantly lower than discrimination thresholds for static circular GPs (1 frame) (mean: 30%; SD: 9.69%) ($t_{(19)} = 5.53$, $p < 0.001$; *Cohen's d*[1] = 2.7). The same significant difference was obtained when comparing dynamic translational GPs (12 frames; 60 Hz) (mean: 24%; SD: 9.25%) with static translational GPs (1 frame) (mean: 37%; SD: 11.36%) ($t_{(19)} = 6.28$, $p < 0.001$; *Cohen's d* = 2.7).

Figure 2 shows the discrimination thresholds for circular and translational GPs for each experimental condition (Table 1). A Shapiro-Wilk test found that residuals for both circular and translational GPs were normally distributed ($p = 0.5$ and $p = 0.6$, for circular and translational GPs, respectively). A two-way repeated measures ANOVA including as within-subjects factors the GP type (circular vs. translational) and the temporal condition (i.e., number of unique frames and pattern update rate) showed a significant effect of the GP type ($F_{(1,19)} = 15.67$, $p < 0.001$, *partial-*$\eta^2 = 0.45$), a significant effect of the temporal condition ($F_{(8,152)} = 12.67$, $p < 0.001$, *partial-*$\eta^2 = 0.4$), but not a significant interaction between GP type and temporal condition ($F_{(8,152)} = 1.059$, $p = 0.3$, *partial-*$\eta^2 = 0.05$). For GP type, circular GPs had always lower discrimination thresholds than translational GPs across all the conditions tested. Post hoc *t-test* comparisons corrected with False Discovery Rate (FDR) with α=0.05 (Benjamini & Hochberg, 1995) between the different conditions are reported in Table 2.

[1] The *Cohen's d* was calculated dividing the mean difference of the two conditions (i.e., static and dynamic GPs) for the difference of the standard deviation of the two conditions: *Cohen's d* = (mean2 - mean1)/SD2-SD1.

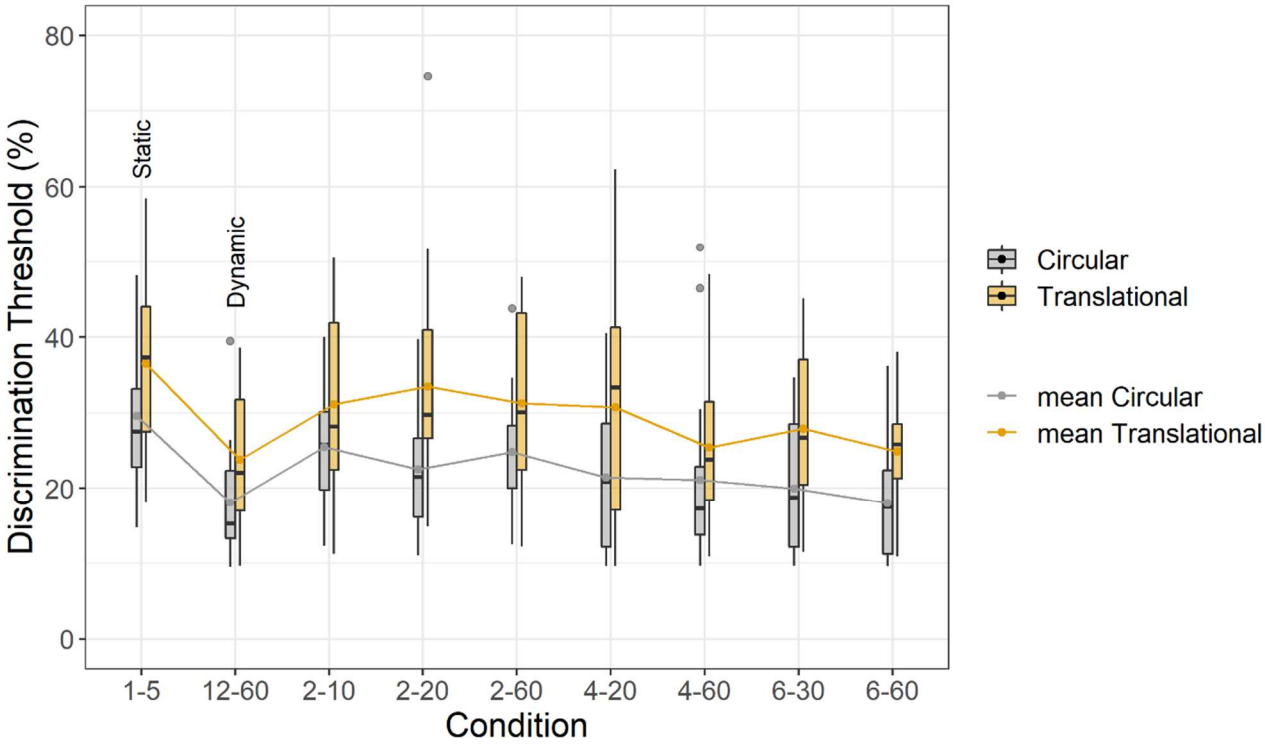

Figure 2. Boxplots of discrimination thresholds (%) of the two experiments with circular (grey bars) and translational (dark yellow bars) GPs. The x-axis reports the nine conditions used in the experiments: number of unique frames and pattern update rate of the GPs. For each boxplot, the horizontal black line indicates the median, the lower and upper hinges correspond to the first and third quartiles (i.e., the 25th and 75th percentiles). Instead, the dot within each boxplot represents the mean discrimination threshold. The upper whisker extends from the hinge to the largest value no further than 1.5 * IQR of the hinge (where IQR is the inter-quartile range or distance between the first and third quartiles). The lower whisker extends from the hinge to the smallest value at most 1.5 * IQR of the hinge.

Circular GPs								
Conditions	**1-5**	**12-60**	**2-10**	**2-20**	**2-60**	**4-20**	**4-60**	**6-30**
12-60	0.0002***							
2-10	0.1037	0.0014***						
2-20	0.0024**	0.0693	0.0649					
2-60	0.0344**	0.0020**	0.6336	0.1466				
4-20	0.0001***	0.1477	0.0267*	0.4164	0.0826			
4-60	0.0014***	0.3344	0.0667	0.3344	0.1124	0.7729		
6-30	0.0002***	0.2053	0.0003***	0.1281	0.0031**	0.3344	0.6336	
6-60	0.0001***	0.9603	0.0002***	0.0015***	0.0006***	0.0201*	0.0482*	0.2743

Table 2. Summary of the FDR adjusted *p*-values for multiple post hoc comparisons between the different temporal conditions of the experiment (the first digit indicates the number of unique frames in the sequence, whereas the second digit the pattern update rate). The asterisks indicate significant comparisons (*p < 0.05, **p < 0.01, ***p < 0.001).

For translational GPs, FDR post hoc comparisons are reported in Table 3.

Translational GPs								
Conditions	**1-5**	**12-60**	**2-10**	**2-20**	**2-60**	**4-20**	**4-60**	**6-30**
12-60	0.0002***							
2-10	0.1532	0.0470*						
2-20	0.4615	0.0141**	0.0644					
2-60	0.0223*	0.0200*	10.000	0.4998				
4-20	0.1265	0.0470*	10.000	0.6044	0.9728			
4-60	0.0034**	0.6044	0.0200*	0.0367*	0.0647	0.1982		
6-30	0.0034**	0.0647	0.2051	0.1194	0.1532	0.3894	0.4344	
6-60	0.0006***	0.7482	0.0373*	0.0223*	0.0200*	0.0470*	0.9675	0.1177

Table 3. Summary of the FDR adjusted *p*-values for multiple post-hoc comparisons between the different conditions. The asterisks indicate the significant comparisons (significance levels: *p < 0.05, **p < 0.01, ***p < 0.001).

To assess the relationship between (i) discrimination thresholds and number of unique frames and (ii) the relationship between discrimination thresholds and GPs' update rate, data were fitted with three different functions: a power law function, an exponential function, and a linear function. The aim was to test which model better described the data and whether there were differences in model's parameters between circular and translational GPs (see the Supplementary Material for the fitting procedure and model selection). We found that for both translational and circular GP, discrimination thresholds were best modelled by a power law function of the form:

$$y = ax^{-b} \quad \text{Eq. 3}$$

where a is the scale parameter and b is the power law exponent.

Once selected the best fitting model (i.e., the power law function), we created and fitted a lattice of power law functions to discrimination thresholds. The lattice of models ranged from a fully saturated model with four parameters (one a and b parameter per GP type) to a maximally restricted model with only two parameters (a and b). Between the fully saturated model and the maximally restricted model, a lattice of models with three parameters were fitted (see the Supplementary Material for more details). We found that a restricted model consisting of different parameters a across the two GP types, but the same power law exponent (b) was the best fitting model. The selected model had the following form:

$$f1(x) = a1x^{-b} \quad \text{Eq. 4}$$
$$f2(x) = a2x^{-b}$$

where $f1(x)$ indicates the function fitted to the circular GPs and $f2(x)$ indicates the function fitted to translational GPs. The model consists of different parameters a (i.e., $a1$ and $a2$) across the two GP types, but the same power law exponent b (Figure 3). For the number of unique frames, restricted model 2 had the following estimated parameters: $a1$ = 27.94 (SE: 0.84), $a2$ = 36.73 (SE: 0.97), b = 0.191 (SE: 0.019) ($quasi$-R^2 = 0.92), whereas for the pattern update rate restricted model 2 had the following parameters: $a1$ = 34.35 (SE: 2.88), $a2$ = 45.24 (SE: 3.63), b = 0.132 (SE: 0.024) ($quasi$-R^2 = 0.79).

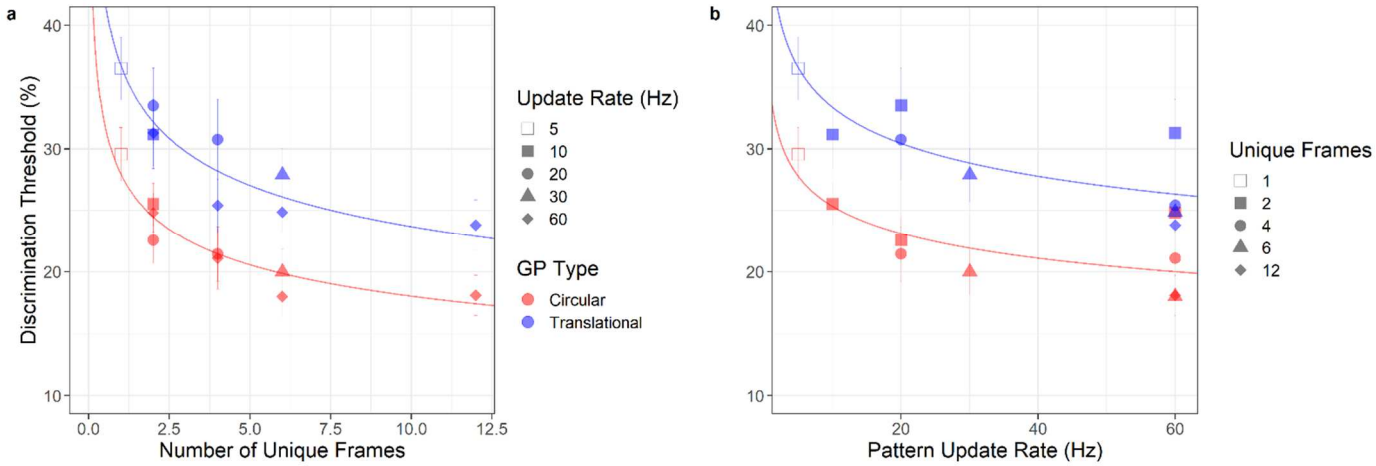

Figure 3. (**a**) Discrimination thresholds as a function of the number of unique frames for circular (red symbols) and translational GPs (blue symbols). (**b**) Discrimination thresholds as a function of the pattern update rate for circular and translational GPs. The curves represent the best fitting model to the data (i.e., Restricted Model 2 [Eq. 4], see the Supplementary Material). Error bars ±SEM.

4.2. Slopes

The slopes give information about the reliability of the estimated discrimination thresholds. Low values of the slopes are related to a smooth psychometric function, indicating higher uncertainty in discrimination of the visual stimuli. A two-way repeated measures ANOVA on the slopes including as within subjects factors the GP type and the temporal condition did not report any significant effect or interaction (GP type: $F_{(1,19)} = 0.008$, $p = 0.9$, *partial-*$\eta^2 = 0.001$; temporal condition: $F_{(8,152)} = 0.39$, $p = 0.9$, *partial-*$\eta^2 = 0.02$; interaction between GP type and temporal condition: $F_{(8,152)} = 1.56$, $p = 0.1$, *partial-*$\eta^2 = 0.08$) (Figure 4).

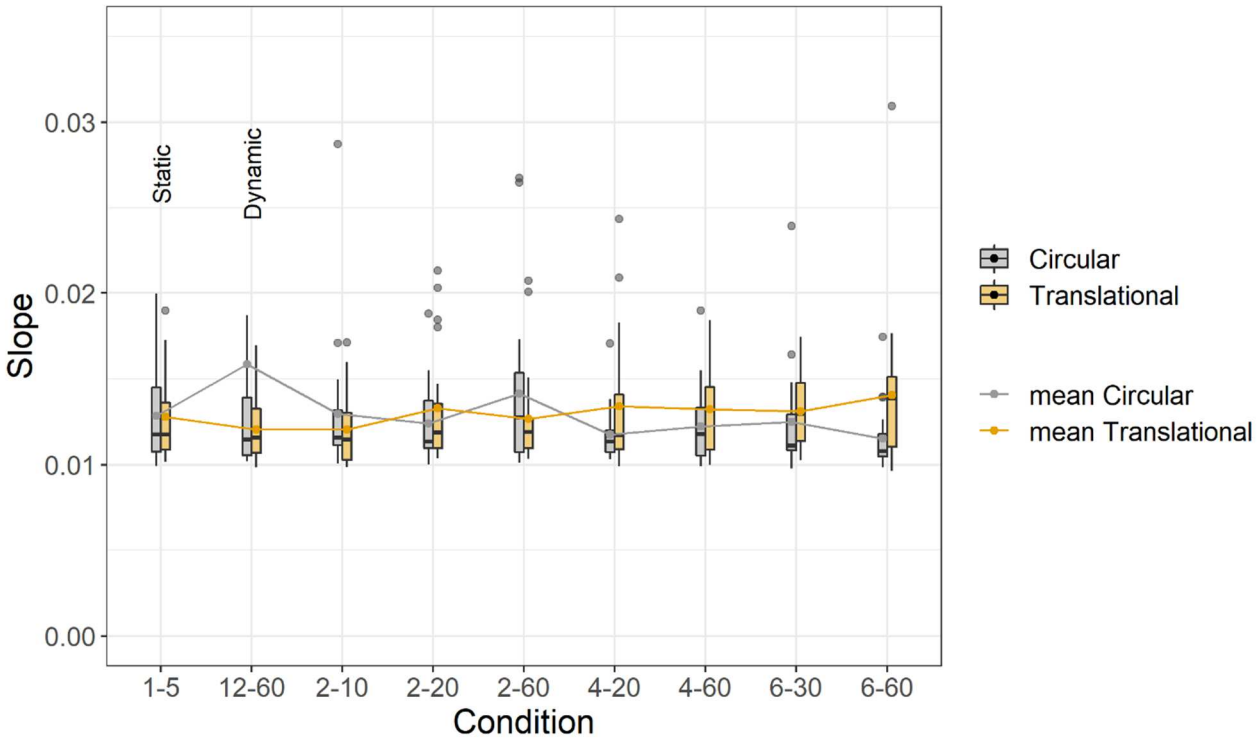

Figure 4. Boxplots of the slopes. The x-axis reports the nine conditions used during the experiment: number of unique frames and pattern update rate of the GPs. For each boxplot, the horizontal black line indicates the median, the lower and upper hinges correspond to the first and third quartiles (i.e., the 25th and 75th percentiles).

5. Discussion

The present study investigated how the human visual system discriminates simple and complex apparent and non-directional motion generated by translational and circular GPs. We measured discrimination thresholds and slopes for circular and translational GPs by varying the number of unique frames composing the pattern and the relative update rates. Our results show that (i) circular GPs are more easily discriminated than translational GPs; (ii) translational and circular GPs are influenced equally by both the number of unique frames and the pattern update rate; it is

not only the pattern update rate but also the number of unique frames that influences the observer's perception of GPs; (iii) dynamic translational and circular GPs are perceived better than the static GPs; (iv) there are no differences between slopes across all the temporal conditions tested, indicating that only the coherence threshold was affected by the temporal manipulations (in terms of number of unique frames and pattern update rate) but not the overall sensitivity of the system.

The evidence that the human visual system shows higher sensitivity to circular GPs than translational GPs is in line with previous psychophysical works (Nankoo et al., 2012; Rampone & Makin, 2020; Wilson & Wilkinson, 1998). For example, Rampone and Makin (2020) performed a study exploring the human brain responses for static translational, circular, and radial GPs by using electroencephalogram (EEG) and event-related potentials (ERPs). The authors examined the trend of the sustained posterior negativity (SPN), an ERP component associated with the perceptual goodness of specific geometric configurations. Participants showed a similar SPN for circular and radial static GPs with respect to translational GPs that were, in turn, the most difficult to detect. Interestingly, other studies found similar results with directional motion (Freeman & Harris, 1992; Lee & Lu, 2010). In particular, Lee and Lu (2010) compared participants' coherence thresholds for circular, radial and translational motion. The results showed greater sensitivity to complex motion than to translational motion and named this phenomenon as "*the complexity advantage*". This result was in line with a previous study by Freeman and Harris (1992), that found that circular and radial RDKs were easier to detect than translational RDKs. However, other studies with RDKs showed contrasting results (Ahlstrom & Borjesson, 1996; Bertone & Faubert, 2003). For example, Bertone and Faubert (2003) using second-order motion (i.e., when the moving contour is defined by qualities that does not result in an increase in luminance or motion energy in the Fourier spectrum of the stimulus [e.g., contrast, texture, flicker, etc.]; Cavanagh & Mather, 1989; Chubb & Sperling, 1988), showed that participants were more sensitive to translational RDKs than circular and radial RDKs. On the other hand, other studies did not find any difference in detection thresholds for translational, radial, and circular RDKs (Blake & Aiba, 1998; Morrone et al., 1995). Therefore, more psychophysical studies are necessary to further investigate how the human visual system detects and discriminates simple and complex motion.

In the present study, we also assessed the relationship between participants' discrimination thresholds and the two independent variables manipulated: the number of unique frames and pattern update rate. We showed that discrimination thresholds decrement for both GP types is better described by a power law function with different scale parameters (a) but same power law exponent (b). Therefore, the best fitting model describing our data supports the presence of a power relationship between discrimination thresholds and number of unique frames and between

discrimination thresholds and pattern update rate, and not a linear relationship as assumed by Nankoo et al. (2015), though in their Figure 3 (page 33) the relationship between detection thresholds and number of unique frames and between detection thresholds and pattern update rates is likely to be either power or exponential. Our results suggest that the form signal contained in each unique frame and the pattern update rate equally contribute to shape the perception of translational and circular GPs. Additionally, the best fitting model shows that discrimination thresholds start at a lower value for circular GPs than for translational GPs (see Figure 3 and the Supplementary Material), but the rate at which the power law function reaches the lower discrimination threshold is the same for the two GP types. In general, observers better discriminated circular GPs than translational GPs, though coherence thresholds decreased at the same rate for both GP types as increasing the number of unique frames and pattern update rate.

Furthermore, looking at Figure 3, it could be observed that it is not only the pattern update rate important for the perception of GPs, as previously stated by Day and Palomares (2014), but also the number of unique frames that forms the pattern plays an important role. In particular, we showed that discrimination thresholds in correspondence to the condition with two unique frames do not vary across the different update rates (i.e., 10, 20, and 60 Hz – see Table 1), for both GP types. Therefore, it seems that discrimination thresholds do not vary with the pattern update rate if the same spatial information is present in the visual stimulus. Moreover, looking at the four conditions with a pattern update rate of 60 Hz (i.e., with 2, 4, 6, and 12 unique frames – Table 1), the lower detection thresholds were estimated with the highest number of unique frames used (i.e., 6 and 12 unique frames) in both GP types. These results might reflect a short integration window between 100 and 200 ms, perhaps comprising the time over which form information is integrated. In general, this may suggest the existence of mechanisms of spatial/form integration in dynamic translational and circular GPs that, along with the pattern update rate, play a fundamental role in the perception of this class of visual textures (Day & Palomares, 2014; Nankoo et al., 2015; Ross et al., 2000).

Finally, our study shows also higher discrimination thresholds for static circular and translational GPs (1 unique frame, 5 Hz) than dynamic GPs, regardless of the temporal condition. Nankoo et al. (2015) argued that this is due to the spatial summation of form signals from all the independent frames composing the dynamic GP. As previously reported, we found that lower discrimination thresholds were obtained with the highest update rate used (i.e., 60 Hz) and with the highest number of unique frames (i.e., 12) that formed the dynamic GPs. Therefore, we argue that both translational and circular dynamic GPs are processed according to a spatial and temporal summation process. Besides, Burr (1980) argued that the temporal summation in a dynamic visual

stimulus leads to significant signal improvements to noise levels. Day and Palomares (2014) found an inverse relationship between the pattern update rate and the participants' detection thresholds; as the pattern update rate increased, observers' detection threshold decreased. The authors showed that the visual system integrates both temporal and orientation signals to improve the detection of ambiguous motion, such as the apparent and non-directional motion generated by dynamic GPs. A possible explanation of this phenomenon could be attributed to the formation of *motion streaks* (Geisler, 1999). Over time, summation of responses to a moving visual object, when it is moving with adequate speed, produces "*speed lines*" or "*motion streaks*" that extend backwards across the retina from the object and display the character of the movement (Burr, 1980; Burr & Ross, 2002), due to temporal integration (Geisler, 1999). Motion streaks aligned to the direction of motion aid the observer to identify a trajectory of a moving object (Apthorp, Schwarzkopf, Kaul, Bahrami, Alais, & Rees, 2013; Geisler, 1999) or the axis of apparent and non-directional motion in the case of dynamic translational GPs (Ross et al., 2000). This phenomenon indicates that the orientation/form signal contributes to the perception of apparent motion. In line with this evidence, the current study shows that both the orientation/form signals and the temporal signals (i.e., generated by the update rate) are integrated to shape the perception of the apparent and non-directional motion in both GP types.

In summary, our results indicate that perception of apparent and non-directional motion evoked by dynamic complex and simple GPs is strongly and equally influenced by temporal and form summation mechanisms in which dipoles' orientation information is summed across frames. The human visual system integrates form and temporal information to shape the perception of non-coherent motion in dynamic GPs. Additionally, the difference in the discrimination thresholds between translational and circular GPs further confirms that different form and motion integration processes subserve the perception of complex and simple global shapes.

6. Conclusion

Apparent and non-directional motion generated by dynamic translational and circular GPs seems to be processed by a wide range of low- and high-level visual areas (Krekelberg et al., 2005; Ostwald et al., 2008). We showed that form and motion processing in dynamic circular and translational GPs interact. We partially replicated the study of Nankoo et al. (2015) showing that dynamic GPs are easier to discriminate than static configurations. This occurs not only because of the spatial summation of the form signals from unique frames but also because of temporal summation. Moreover, we extended the findings of Nankoo et al. (2015) by assessing the role of the number of unique frames and the pattern update rate in circular GPs. Interestingly, we found that

both these variables play the same role in translational and circular GPs. We conclude that it is not only the pattern update rate that aids the discrimination of apparent and non-directional motion from translational and circular GPs (Day & Palomares, 2014), but it also depends on the amount of form signals that are summed by the visual system over the frames.

Acknowledgements

This work was carried out within the scope of the project "Use-inspired basic research", for which the Department of General Psychology of the University of Padova has been recognized as "Dipartimento di Eccellenza" by the Ministry of University and Research. This study was supported by the University of Padova, Department of Psychology and by the Human Inspired Centre. Jorge Almeida is supported by a European Research Council (ERC) Starting Grant under the European Union's Horizon 2020 research and innovation programme (Grant# 802553 - ContentMAP). The authors thank Proaction Laboratory and University of the Coimbra for the support in carrying out the present research and Dr Adriano Contillo for his helpful suggestions on the fitting procedure for data analysis.

Conflict of interest

The authors declare no competing financial interests.

Author contribution

Rita Donato, Andrea Pavan: Conceptualization and Methodology. **Andrea Pavan:** Software. **Rita Donato:** Data collection. **Rita Donato, Andrea Pavan:** Data curation. **Rita Donato, Andrea Pavan:** Data analysis. **Rita Donato, Andrea Pavan:** Writing, Original draft preparation. **Andrea Pavan, Gianluca Campana:** Supervision. **Rita Donato, Andrea Pavan, Gianluca Campana:** Writing- Reviewing and Editing. **Massimo Nucci, Jorge Almeida:** Reviewing and Editing.

References

Anderson, S. J., & Swettenham, J. B. (2006). Neuroimaging in human amblyopia. *Strabismus*, *14*(1), 21–35. doi: 10.1080/09273970500538082

Apthorp, D., Schwarzkopf, D. S., Kaul, C., Bahrami, B., Alais, D., & Rees, G. (2013). Direct evidence for encoding of motion streaks in human visual cortex. *Proceedings. Biological Sciences / The Royal Society*, *280*(1752), 20122339. doi: 10.1098/rspb.2012.2339

Bertone, A., & Faubert, J. (2003). How is complex second-order motion processed? *Vision Research*, *43*(25), 2591–2601. doi: 10.1016/s0042-6989(03)00465-6

Blake, R., & Aiba, T. S. (1998). Detection and discrimination of optical flow components. *Japanese Psychological Research*, *40*(1), 19-30. doi: 10.1111/1468-5884.00071

Burr, D. (1980). Motion smear. *Nature, 284*, 64–165. doi: 10.1038/284164a0

Burr, D. C., & Ross, J. (2002). Direct evidence that "speedlines" influence motion mechanisms. *Journal of Neuroscience, 22*(19), 8661-8664. doi: 10.1523/JNEUROSCI.22-19-08661.2002

Burr, D., & Ross, J. (2006). The effects of opposite-polarity dipoles on the detection of Glass patterns. *Vision Research*, *46*(6–7), 1139–1144. doi: 10.1016/j.visres.2005.09.018

Cavanagh, P., & Mather, G. (1989). Motion: the long and short of it. *Spatial Vision, 4*(2–3), 103–129. doi:10.1163/156856889X00077.

Chubb, C., & Sperling, G. (1988). Drift-balanced random stimuli: A general basis for studying non-Fourier motion perception. Journal of the Optical *Society of America, 5*(11), 1986–2007. doi:10.1364/JOSAA.5.001986.

Dakin, S. C., & Bex, P. J. (2002). Summation of concentric orientation structure: Seeing the Glass or the window? *Vision Research, 42*(16), 2013–2020. doi: 10.1016/s0042-6989(02)00057-3

Day, A. M., & Palomares, M. (2014). How temporal frequency affects global form coherence in Glass patterns. *Vision Research*, *95*, 18–22. doi: 10.1016/j.visres.2013.11.009

Faul, F., Erdfelder, E., Lang, A.-G., & Buchner, A. (2007). G * Power 3: A flexible statistical power analysis program for the social, behavioral, and biomedical sciences. *Behavior Research Methods*, *39*, 175-191. doi: 10.3758/bf03193146

Faul, F., Erdfelder, E., Buchner, A., & Lang, A.-G. (2009). Statistical power analyzes using G * Power 3.1: Tests for correlation and regression analyzes. *Behavior Research Methods*, *41*, 1149-1160. doi: 10.3758/BRM.41.4.1149

Freeman, T. C., & Harris, M. G. (1992). Human sensitivity to expanding and rotating motion: effects of complementary masking and directional structure. *Vision Research*, *32*(1), 81–87. doi: 10.1016/0042-6989(92)90115-y

Geisler, W. S. (1999). Motion streaks provide a spatial code for motion direction. *Nature, 400*(6739), 65-69. doi: 10.1038/21886

Glass, L. (1969). Moiré Effect from Random Dots. *Nature*, *223*, 578–580. doi: 10.1038/223578a0

Kelly, D. M., Bischof, W. F., Wong-Wylie, D. R., & Spetch, M. L. (2001). Detection of glass patterns by pigeons and humans: implications for differences in higher-level processing. *Psychological Science*, *12*(4), 338–342. doi: 10.1111/1467-9280.00362

Kourtzi, Z., Krekelberg, B., & van Wezel, R. J. A. (2008). Linking form and motion in the primate brain. *Trends in Cognitive Sciences*, *12*(6), 230–236. doi: 10.1016/j.tics.2008.02.013

Kourtzi, Z., Vatakis, A., & Krekelberg, B. (2005). Global motion from form in the human visual cortex. *Journal of Vision*, *5*(8), 1063. http://journalofvision.org/5/8/1063/

Krekelberg, B., Vatakis, A., & Kourtzi, Z. (2005). Implied motion from form in the human visual cortex. *Journal of Neurophysiology, 94*(6), 4373–4386. doi: https://doi.org/10.1167/5.8.1063

Krekelberg, B., Dannenberg, S., Hoffmann, K.-P., Bremmer, F., & Ross, J. (2003). Neural correlates of implied motion. *Nature*, *424*(6949), 674–677. doi: 10.1038/nature01852

Lee, A. L., & Lu, H. (2010). A comparison of global motion perception using a multiple-aperture stimulus. *Journal of Vision*, *10*(4), 1–16. doi: 10.1167/10.4.9

Levitt, H. (1971). Transformed Up-Down Methods in Psychoacoustics. *Journal of the Acoustical Society of America, 49*(2), 467+. doi: https://doi.org/10.1121/1.1912375

Lewis, T. L., Ellemberg, D., Maurer, D., Wilkinson, F., Wilson, H. R., Dirks, M., & Brent, H. P. (2002). Sensitivity to global form in Glass patterns after early visual deprivation in humans. *Vision Research*, *42*(8), 939–948. doi: 10.1016/s0042-6989(02)00041-x

Mayr, S., Erdfelder, E., Buchner, A., & Faul, F. (2007). A short tutorial of GPower. *Tutorials in Quantitative Methods for Psychology, 3*(2), 51-59. doi: 10.20982/tqmp.03.2. p051

Mather, G., Pavan, A., Bellacosa Marotti, R., Campana, G., & Casco, C. (2013). Interactions between motion and form processing in the human visual system. *Frontiers in Computational Neuroscience, 7*, 65. doi: 10.3389/fncom.2013.00065

Mather, G., Pavan, A., Bellacosa, R. M., & Casco, C. (2012). Psychophysical evidence for interactions between visual motion and form processing at the level of motion integrating receptive fields. *Neuropsychologia*, *50*(1), 153-159. doi: 10.1016/j.neuropsychologia.2011.11.013

Morrone, M. C., Burr, D. C., & Vaina, L. M. (1995). Two stages of visual processing for radial and circular motion. *Nature*, *376*(6540), 507–509. doi: 10.1038/376507a0

Nankoo, J. F., Madan, C. R., Spetch, M. L., & Wylie, D. R. (2012). Perception of dynamic Glass patterns. *Vision Research*, *72*, 55–62. doi: 10.1016/j.visres.2012.09.008

Nankoo, J. F., Madan, C. R., Spetch, M. L., & Wylie, D. R. (2015). Temporal summation of global form signals in dynamic Glass patterns. *Vision Research*, *107*, 30–35. doi: 10.1016/j.visres.2014.10.033

Or, C. C. F., Khuu, S. K., & Hayes, A. (2007). The role of luminance contrast in the detection of global structure in static and dynamic, same- and opposite-polarity, Glass patterns. *Vision Research*, *47*(2), 253–259. doi: 10.1016/j.visres.2006.10.010

Ostwald, D., Lam, J. M., Li, S., & Kourtzi, Z. (2008). Neural coding of global form in the human visual cortex. *J Neurophysiol*, *99*(5), 2456–2469. doi: 10.1152/jn.01307.2007

Pavan, A., Hobaek, M., Blurton, S. P., Contillo, A., Ghin, F., & Greenlee, M. W. (2019). Visual short-term memory for coherent motion in video game players: evidence from a memory-masking paradigm. *Scientific Reports, 9*, 6027. doi: 10.1038/s41598-019-42593-0

Pavan, A., Bimson, L. M., Gall, M. G., Ghin, F., & Mather, G. (2017). The interaction between orientation and motion signals in moving oriented Glass patterns. *Visual Neuroscience*, *34*, E010. doi: 10.1017/S0952523817000086

Pavan, A., Contillo, A., Ghin, F., Foxwell, M. J., & Mather, G. (2019). Limited attention diminishes spatial suppression from large field Glass patterns. *Perception, 48*(4), 286-315. doi: 10.1177/0301006619835457

Pavan, A., Ghin, F., Donato, R., Campana, G., & Mather, G. (2017). The neural basis of form and form-motion integration from static and dynamic translational Glass patterns: A rTMS investigation. *NeuroImage*, *157*, 555-560. doi: 10.1016/j.neuroimage.2017.06.036

Pavan, A., Marotti, R. B., & Mather, G. (2013). Motion-form interactions beyond the motion integration level: evidence for interactions between orientation and optic flow signals. *Journal of Vision*, *13*(6). doi: 10.1167/13.6.16. PMID: 23729767

Rampone, G., & Makin, A. D. J. (2020). Electrophysiological responses to regularity show specificity to global form: The case of Glass patterns. *European Journal of Neuroscience*. doi: 10.1111/ejn.14709

Ross, J. (2004). The perceived direction and speed of global motion in Glass pattern sequences. *Vision Research*, *44*(5), 441–448. doi: 10.1016/j.visres.2003.10.002

Ross, J., Badcock, D. R., & Hayes, A. (2000). Coherent global motion in the absence of coherent velocity signals. *Current Biology*, *10*(11), 679–682. doi: 10.1016/s0960-9822(00)00524-8

Shen, Y. (2013). Comparing adaptive procedures for estimating the psychometric function for an auditory gap detection task. *Attention, Perception, and Psychophysics*, *75*(4). doi: 10.3758/s13414-013-0438-9

Wilson, H. R., & Wilkinson, F. (1998). Detection of global structure in Glass patterns: Implications for form vision. *Vision Research*, *38*(19), 2933–2947. doi: 10.1016/s0042-6989(98)00109-6

Wilson, H. R., Wilkinson, F., Dakin, S. C., & Bex, P. J. (2003). Further evidence for global orientation processing in circular Glass patterns (multiple letters). *Vision Research, 43*(5), 563–566. doi: 10.1016/s0042-6989(02)00651-x

Wilson, J. A., Switkes, E., & de Valois, R. L. (2004). Glass pattern studies of local and global processing of contrast variations. *Vision Research*, *44*(22), 2629–2641. doi: 10.1016/j.visres.2003.06.001

World Medical Association, 2013. World Medical Association Declaration of Helsinki. Ethical Principles for Medical Research Involving Human Subjects. *JAMA, 310*, 2191–2194. doi: 10.1001/jama.2013.281053